PETROLOGY AND GEOCHEMISTRY OF THE ENRICHED POIKILITIC SHERGOTTITE NORTHWEST AFRICA 10169: INSIGHT INTO THE MARTIAN INTERIOR. L. M. Combs[1], A. Udry[1], G. H. Howarth[2], T. J. Lapen[3], M. Righter[3], J. Gross[4], J. M. D. Day[5], and R. R. Rahib[1], [1]Department of Geoscience, University of Nevada Las Vegas, 4505 S. Maryland Pkwy, Las Vegas NV 89154-4010 (combsl1@unlv.nevada.edu), [2]Department of Geology, University of Georgia, Athens GA 30602-2501, [3]Department of Geosciences, University of Houston, Houston TX 77204-5007, [4]Department of Earth & Planetary Sciences, Rutgers University, Piscataway NJ 08854, [5]Scripps Institution of Oceanography, University of California San Diego, La Jolla CA 92093-0244.

Introduction: Shergottites are the most abundant group of martian meteorites, and are divided into basaltic, olivine-phyric, poikilitic, and gabbroic petrologic types. [e.g., 1, 2]. Shergottites are also divided into three geochemical groups (enriched, intermediate, and depleted) based upon their relative light rare earth element (LREE) enrichment, and source ε^{143}Nd and ε^{176}Hf compositions [e.g., 1, 3]. These variations have arisen through the sampling of distinct geochemical reservoirs, whose origins and locations remain controversial [e.g., 4, 5]. The crystallization ages of the shergottites, dated using the Sm-Nd, Lu-Hf, and Rb-Sr isotope systems, mainly range from ~150-574 Ma [e.g., 6, 7, 8], with two meteorites as old as ~2.4 Ga [9, 10]. Here we present new major, minor and trace element compositions; oxygen fugacity (fO_2), temperature and pressure calculations; and Lu-Hf ages and isotopic composition of Northwest Africa (NWA) 10169. NWA 10169 is a poikilitic shergottite that was found in the Laayoune region of Western Saraha in 2015. Our data indicate that NWA 10169 is a new member of the enriched shergottites.

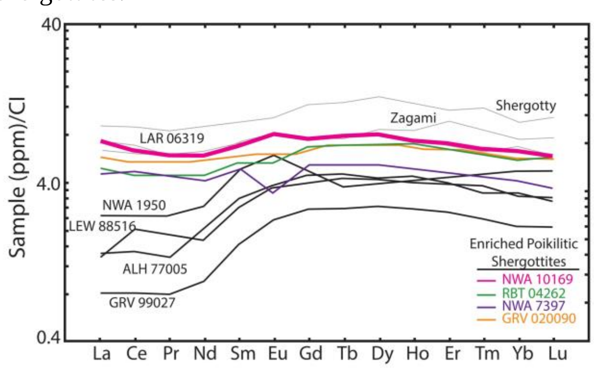

Figure 1. The measured bulk REE profile of NWA 10169 in comparison to previously studied shergottites. Figure modified from [11]; and references therein.

Analytical Techniques: Major, minor, and trace element *in situ* compositional analyses were performed using the *JEOL JXA-8900* electron microprobe (EMP) at UNLV, and the *New Wave Research UP213* (213nm) solid-state laser ablation system coupled to a *ThermoScientific iCAP Qc* ICP-MS at the Scripps Institute of Oceanography (SIO). Bulk major, minor, and trace element compositions were obtained on a second *ThermoScientific iCAP Qc* ICP-MS housed at SIO.

Lu-Hf Crystallization Age Dating. A ~1 g sample of NWA 10169 was crushed in a clean agate mortar and pestle. A pyroxene fraction was hand-picked from the powder; while spinel, and maskelynite-rich fractions were isolated through density separation, using thallium malonate (~4.36 g/cc) and lithium metatungstate (~2.75 g/cc), respectively. The mineral separates, a bulk <45 µm sample, and a bulk (minus separates) sample were dissolved through microwave digestion, then 4-stage column chemistry was performed, isolating Lu and Hf. All samples were analyzed using a *Nu Instruments Nu-Plasma II* MC-ICP-MS at the University of Houston.

Petrography and Mineral Chemistry: NWA 10169 exhibits the characteristic bimodal texture observed in the poikilitic shergottites. The namesake poikilitic texture manifests as large (up to 4 mm), anhedral pyroxene oikocrysts, enclosing anhedral olivine (100-800 µm) and anhedral to subhedral chromite (25-100 µm) chadacrysts. The pyroxene oikocrysts show sharp compositional boundaries from pigeonite cores ($Wo_6En_{68}Fs_{27}$) and mantles ($Wo_9En_{64}Fs_{18}$), to augite rims ($Wo_{35}En_{47}Fs_{18}$). Olivine chadacrysts range from Fo_{68} to Fo_{61} from the cores to the rims of the oikocrysts. Chromite chadacrysts have uniform compositions of $Chr_{66}Mgn_6Spn_{15}Ulv_{12}$. Interstitial to the poikilitic textures, is a relatively more equigranular assemblage of subhedral pyroxene (500-1000 µm), subhedral to euhedral olivine (~800 µm), and plagioclase that has been completely shocked to maskelynite (500-100 µm). Anhedral spinel (up to 300 µm) are commonly enclosed by olivine, and there are minor phosphates, pyrrhotite, and ilmenite present. This texture is heretofore referred to as non-poikilitic. Non-poikilitic pyroxene exists as discrete grains of pigeonite ($Wo_{10}En_{59}Fs_{31}$) and augite ($Wo_{33}En_{47}Fs_{20}$). Non-poikilitic pyroxene also shows significantly higher concentrations of incompatible elements (Ti, Y, Zr) than poikilitic pyroxene. Non-poikilitic olivine is more Fe-rich (Fo_{60}) than the olivine chadacrysts. Maskelynite in the non-poikilitic texture range from An_{36} to An_{51}, and show positive Eu anomalies [Eu/Eu* = 3.4]. Spinel in the non-poikilitic textures are more Ti-rich ($Chr_{32}Mgn_{11}Spn_8Ulv_{50}$) than the poikilitic chromite. Merrillite in NWA 10169, though only in trace amounts, exert an important control on the bulk REE composition with La ~555xCI.

Geochemical Classification: Bulk REE concentrations of NWA 10169, normalized to CI, show a relatively flat, LREE enriched [$(La/Yb)_{CI}$ = 1.18] profile (Fig. 1). The profile has a similar pattern to previously studied enriched poikilitic shergottites [11-13], and shows one of the highest REE-enrichments in the shergottite suite. This observation, along with the textural and compositional characteristics of NWA 10169 has led to its classification as a new member of the geochemically enriched poikilitic shergottites.

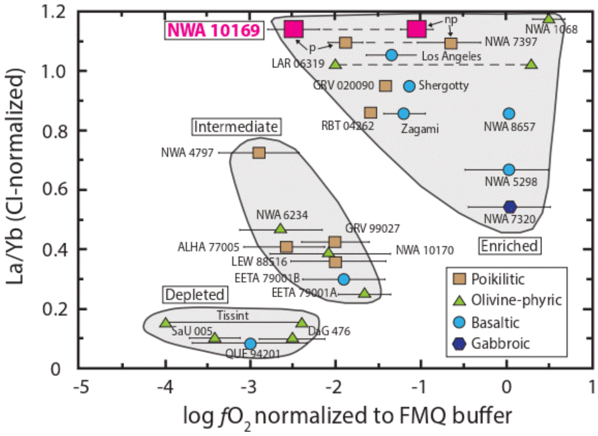

Figure 2. fO_2 normalized to FMQ against the degree of LREE enrichment $(La/Yb)_{CI}$ in NWA 10169 and other shergottites. Np = non-poikilitic, p = poikilitic. Figure modified from [14] and references therin.

Conditions of Formation: The positive correlation between pressure and Ti/Al ratios in pyroxene has been experimentally calibrated for martian meteorites [15, 16], and has been used to estimate pressures of pyroxene oikocryst formation in enriched poikilitic shergottites [11]. Pyroxene Ti/Al ratios in NWA 10169 suggest pressures of >9 kbar during oikocryst formation. The non-poikilitic texture likely crystallized at shallower depths, as the relatively finer and more equigranular texture is consistent with faster cooling at lower pressures. Subsolidus equilibration temperature and fO_2 were calculated for both the poikilitic and non-poikilitic textures using the olivine-pyroxene-spinel oxygeobarometer and olivine-spinel geothermometer [17]. The poikilitic texture yielded a temperature of 994 ± 22^{0}C and a logfO_2 of FMQ -2.50 ± 0.38, while the non-poikilitic texture yielded a temperature of 803 ± 66^{0}C and a logfO_2 of FMQ -1.08 ± 0.15 (Fig. 2). The compositional differences between the poikilitic and non-poikilitic textures, and these results, suggest a formation consistent with the polybaric crystallization model proposed by [11]; in which the poikilitic texture likely formed at depth, under more reducing conditions and pressures >9 kbar, and following magma ascent, the non-poikilitic texture began to form at shallower depths and under more oxidizing conditions.

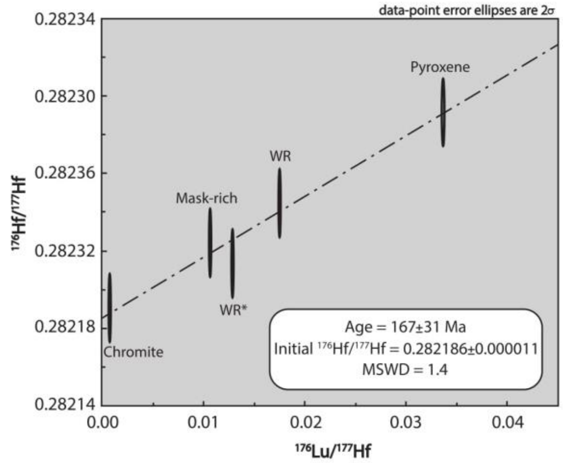

Figure 3. Lu-Hf isochron for NWA 10169, calculated with *Isoplot*. Mask = maskelynite; WR = whole rock; WR* = whole rock minus mineral separates.

Lu-Hf Age and Source Composition: A 5 point Lu-Hf isochron yielded a crystallization age of 167 ± 31 Ma (2σ, MSWD = 1.4) for NWA 10169, and a derived initial $^{176}Hf/^{177}Hf$ of 0.282186 ± 0.000011 (Fig. 3). The crystallization age lies between the youngest (~150 Ma) and oldest (~225 Ma) enriched poikilitic shergottites, NWA 4468 [18] and RBT 04262 [19], respectively. The calculated source $^{176}Lu/^{177}Hf$ of 0.02748 ± 0.00037 is identical to the calculated sources of NWA 4468 and RBT 04262, basaltic shergottites Shergotty and Zagami, and olivine-phyric shergottite LAR06319, suggesting a shared mantle source for this group of enriched shergottites.

References: [1] Bridges J. C. and Warren P. H. (2006) *Journal of the Geological Soc., 163*, 229-251. [2] Filiberto J. et al. (2014) *Amer. Mineralogist, 99*, 601-606. [3] DeBaille V. et al. (2008) *EPSL, 269*, 186-199. [4] Herd C. D. K. et al. (2002) *GCA, 66*, 2025-2036. [5] Peters T. J. et al. (2015) *EPSL, 418*, 91-102. [6] Nyquist L. E. et al. (2001) *SSSI, 12*, 105-164. [7] Brennecka G. A. et al. (2014) *Meteoritics & Planet. Sci., 49*, 412-418. [8] Shafer J. T. et al. (2010) *GCA, 74*, 7307-7328. [9] Lapen T. J. et al. (2017) *Sci. Advances, 3*, e1600922. [10] Herd C. D. K. et al. (2017) *GCA, 218*, 1-26. [11] Howarth G. H. et. al. (2014) *Meteoritics & Planet. Sci., 49*, 1812-1830. [12] Usui T. et al. (2010) *GCA, 74*, 7283-7306. [13] Jiang Y. and Hsu W. (2012) *Meteoritics & Planet. Sci., 47*, 1419-1435. [14] Howarth G. H. et al. (2017) *Meteoritics & Planet. Sci., online.* [15] Nekvasil H. et al. (2004) *Journal of Petrology, 45*, 693-721. [16] Filiberto J. et al. (2010) *Meteoritics & Planet. Sci., 45*, 1258-1270. [17] Sack R. O. and Ghiorso M. S. (1989) *Contrib. to Mineralogy and Petrology, 102*, 41-68. [18] Borg L. E. et al. (2008) *LPSC XXXIX #1851*. [19] Lapen T. J. et al. (2008) *LPSCXXXIX #2073.*